



Research article

Naringenin alleviates liver fibrosis by triggering autophagy-dependent ferroptosis in hepatic stellate cells

Ting Yu^{a,*}, Xuejia Lu^a, Yan Liang^a, Lin Yang^a, Yuehan Yin^b, Hong Chen^{a,**}^a Department of Gastroenterology, Zhongda Hospital, School of Medicine, Southeast University, No. 87 Dingjiaqiao, Nanjing, Jiangsu, 210009, People's Republic of China^b China HuaYou Group Corporation, Beijing, 100724, People's Republic of China

ARTICLE INFO

Keywords:

Liver fibrosis
HSCs
Ferroptosis
Autophagy
Naringenin

ABSTRACT

Inhibition of activated hepatic stellate cells (HSCs) is a promising approach for treating liver fibrosis, and the ferroptosis has emerged as a pivotal mechanism to achieve this inhibition. The effects of naringenin, a flavonoid with anti-inflammatory properties, have not been thoroughly examined in liver fibrosis. Therefore, we used cholestasis model to study the effect of naringenin on liver fibrosis. Our findings demonstrated a significant exacerbation of liver tissue damage and fibrosis in mice subjected to bile duct ligation (BDL), accompanied by a substantial upregulation of fibrogenesis-related gene expression. Notably, naringenin administration markedly alleviated liver injury and fibrosis in these mice. Furthermore, naringenin exhibited inhibitory effects on the activation of HSCs, concurrently inducing ferroptosis. Importantly, naringenin significantly increased autophagic activity in HSCs. This effect was counteracted by co-administration of the autophagy inhibitor 3-MA, leading to a notable reduction in naringenin-induced HSC ferroptosis. In BDL model mice, naringenin demonstrated a mitigating effect on liver fibrosis, suggesting a potential correlation with naringenin-induced ferroptosis of HSCs. These results provide novel insights into the molecular mechanisms of naringenin-induced ferroptosis and highlight autophagy-dependent ferroptosis as a promising therapeutic strategy for liver fibrosis.

1. Introduction

Liver fibrosis represents a burgeoning global health challenge characterized by elevated morbidity and mortality; however, definitive treatment remains elusive [1,2]. This is due to the development of scar tissue following sustained liver injury induced by factors such as viral infections, cholestasis, alcoholic liver disease, and non-alcoholic fatty liver disease, culminating in progression to cirrhosis and hepatocellular carcinoma (HCC) [3]. The development of fibrosis is the result of excessive accumulation of extracellular matrix (ECM), resulting from the activation of hepatic stellate cells (HSCs) [4]. In response to long-term injury, quiescent HSCs undergo a loss of vitamin A content and eventually differentiate into activated myofibroblasts that express alpha-smooth muscle actin (α -SMA) [5]. HSCs in the activated stage continue to generate substantial amounts of collagen 1A1 (COL1A1) and fibronectin, fostering an undue buildup of the ECM [6]. Therefore, targeting activated HSCs to mitigate ECM accumulation is a promising and viable therapeutic approach for hepatic fibrosis [7].

* Corresponding author.

** Corresponding author.

E-mail addresses: 18101595196@163.com (T. Yu), njchenhong66@163.com (H. Chen).

Ferroptosis is an innovative form of programmed cell death distinct from apoptosis, necrosis, or pyroptosis, arising from the uncontrolled accumulation of membrane lipid peroxidation (LPO) in an iron-dependent manner [8,9]. In the process of ferroptosis, mitochondria showed obvious morphological changes, including volume reduction, membrane density compaction, mitochondrial cristae loss and outer membrane rupture [10]. Recent studies have identified multiple triggers of ferroptosis, including disruption of iron metabolism, accumulation of LPO, depletion of glutathione (GSH), inhibition of glutathione peroxidase 4 (GPX4), and deficiency in solute carrier family 7 member 11 (SLC7A11) [11]. It is worth noting that ferroptosis has a complex association with the pathogenesis and regulation of various liver diseases, such as fatty liver, fibrosis, and HCC [5,9,12]. Inducing ferroptosis in activated HSCs is a promising strategy for preventing liver fibrosis. Consequently, the triggering of ferroptosis in activated HSCs has the potential to be a novel treatment approach for hepatic fibrosis. Although current studies have confirmed the ability of induced ferroptosis in activated HSCs to mitigate ECM generation, the underlying molecular mechanisms remain unclear. Furthermore, there is a notable lack of safe and effective ferroptosis inducers for treating liver fibrosis.

Numerous studies have consistently observed an increase in autophagy flux during ferroptosis [13,14]. Therefore, autophagy is considered to be an inducible factor regulating ferroptosis. Appropriate autophagy may be beneficial for cell survival; however, excessive autophagy may cause iron-dependent cell death [15]. The occurrence of ferroptosis and the regulation of iron levels by ferritin are crucial [16]. The autophagy degradation of ferritin, known as ferritinophagy and dependent on nuclear receptor coactivator 4 (NCOA4), is a crucial process [17]. Ferritinophagy results in the breakdown of ferritin, releasing a significant amount of free iron that facilitates the initiation of ferroptosis [18]. The attenuation or inhibition of NCOA4 or ATG hinders ferritinophagy, consequently constraining ferroptosis [19]. Autophagy regulates LPO through various mechanisms. Autophagy is involved in lipid droplet degradation in lysosomes mediated by Rab7A, thus promoting LPO [20,21]. In contrast, chaperone-mediated autophagy triggers ferroptosis through the degradation of GPX4 [22]. Hence, drawing from these findings, it is evident that the activation of autophagy triggers ferroptosis.

Recently, natural product-induced ferroptosis has become a realistic choice for treating liver diseases [23]. Naringenin (4,5,7-trihydroxyflavone), a flavonoid compound abundant in plants, exhibits a spectrum of pharmacological activities, including anti-inflammatory, antitumor, and immunomodulatory effects [24–27]. Although naringenin has demonstrated efficacy in mitigating liver fibrosis induced by carbon tetrachloride, a comprehensive understanding of its underlying mechanisms is lacking [28,29]. In this study, a bile duct ligation (BDL) mouse model was used to investigate the *in vivo* therapeutic effects of naringenin. BDL induces bile acid stasis and creates an inflammatory environment. Excessive bile acid exposure triggers HSC activation, which ultimately results in liver fibrosis. Additionally, we examined the role of naringenin treatment in fostering ferroptosis in HSCs and investigated the associated molecular mechanisms.

2. Materials and methods

2.1. Reagents and antibodies

Naringenin (99% purity, S90147) was purchased from Solarbio Science and Technology Co. Ltd (Beijing, China). Ferrostatin-1 (HY-100579) and 3-Methyladenine (3-MA, HY-19312) were purchased from MedChem Express (Monmouth Junction, NJ, USA). Primary antibodies targeting α -SMA (ab124964), Collagen 1A1 (ab138492), Fibronectin (ab45688), SLC7A11 (ab175186), GPX4 (ab125066), ACSL4 (ab155282), p62 (ab109012), and LC3-I/II (ab128025) were acquired from Abcam Technology (Cambridge, MA, USA). The primary antibody against β -actin (AC026n) was obtained from ABclonal Biotechnology (Wuhan, China). Horseradish peroxidase (HRP) goat anti-mouse IgG (H + L) and HRP Goat Anti-Rabbit IgG (H + L) were supplied by ABclonal. High-sensitivity ECL Western blot substrates were procured from Tanon (Shanghai, China).

2.2. Animals

SPF male C57BL/6 J mice were supplied by Beijing Weitong Lihua Experimental Animal Co., Ltd. (SCXK2012-0001). The mice were provided with standard mouse feed and water following a 12-h light cycle. All experimental protocols adhered to The Animal Ethics Committee of Zhongda Hospital and the 8th edition of the NRC Guide for the Care and Use of Laboratory Animals.

2.3. Bile duct ligation

Forty mice were randomly assigned to four groups: normal, BDL, and naringenin treatment (25, 50, or 100 mg/kg). Random allocation was conducted using <http://www.randomizer.org>, resulting in eight mice per group. All the mice were anesthetized with isoflurane prior to surgery. Under sterile conditions, BDL was performed during midline laparotomy. The common bile duct was exposed and ligated near the liver hilum using 3-0 surgical silk, following established protocols [30]. The normal group underwent sham surgery involving exposure of the common bile duct without ligation. Following bile duct ligation, mice in the naringenin groups received intraperitoneal injections of naringenin at doses of 25, 50, and 100 mg/kg every day for 2 weeks. The mice in the normal and BDL groups received equivalent volumes of normal saline via intraperitoneal injection. Liver tissue was collected under general anesthesia 2 weeks post-surgery.

2.4. Blood biochemical indices and histological examinations

To evaluate the blood parameters, the levels of key biochemical markers, including Aspartate aminotransferase (AST), Alanine Aminotransferase (ALT), and Alkaline Phosphatase (ALP), were measured. The analysis was performed using a TOSHIBA TBA-40FR biochemical analyzer. For histology, the harvested liver tissues were fixed in 4% paraformaldehyde, followed by graded dehydration and embedding in paraffin. Consistent with established methodologies [31], 4 μm -thick liver sections were prepared to staining with H&E, Masson, and Sirius Red.

2.5. Western blot

Samples were resolved on 8–12% SDS-PAGE gels, and the separated proteins were transferred onto nitrocellulose membranes. These membranes were then blocked with 1% BSA for 1 h at 37 °C and subsequently incubated with specific antibodies overnight at 4 °C. Following primary antibody incubation, membranes were probed with HP-conjugated secondary antibodies. The protein bands were detected using LumiGLO chemiluminescence substrates obtained from KPL (Guildford, UK). This chemiluminescent reaction facilitates the visualization and quantification of protein bands on nitrocellulose membranes.

2.6. RNA isolation and qPCR

Total RNA was isolated utilizing Trizol Reagent, followed by reverse transcription to generate complementary DNA (cDNA). EvaGreen qPCR MasterMix was used in a Real-Time PCR detection system (Bio-Rad Laboratories, USA). Trizol Reagent facilitated the isolation of total RNA, and reverse transcription converted the extracted RNA into cDNA. Subsequent qPCR analysis, employing EvaGreen qPCR MasterMix, was conducted using a Real-Time PCR detection system (BioRad Laboratories, USA). This approach enables the quantification of specific nucleic acid sequences and assessment of gene expression levels. The sequences of the mouse gene primers were as follows:

Acta2 forward: 5'-GTGTTGCCCTGAAGAGCAT-3';

Acta2 reverse: 5'-GCTGGGACATTGAAAGTCTCA-3'

Col1a1 forward: 5'-GAGGGCCAAGACGAAGACATC-3';

Col1a1 reverse: 5'-CAGATCACGTCATCGCACAAAC-3';

Fn1 forward: 5'-AGGAAGCCGAGGTTTAACTG-3';

Fn1 reverse: 5'-AGGACGCTCATAAGTGTACC-3';

The sequence of human genes primers are as follows:

Acta2 forward: 5'-AAAAGACAGCTACGTGGGTGA-3';

Acta2 reverse: 5'-GCCATGTTCTATCGGGTACTTC-3';

Col1a1 forward: 5'-GTGCGATGACGTGATCTGTGA-3';

Col1a1 reverse: 5'-CGGTGGTTTCTTGGTCGGT-3';

Fn1 forward: 5'-AGGAAGCCGAGGTTTAACTG-3';

Fn1 reverse: 5'-AGGACGCTCATAAGTGTACC-3';

Ptgs2 forward: 5'-CTGGCGCTCAGCCATACAG-3';

Ptgs2 reverse: 5'-CGCACTTATACTGGTCAAATCCC-3';

Gpx4 forward: 5'-GAGGCAAGACCGAAGTAAACTAC-3';

Gpx4 reverse: 5'-CCGAAGTGGTTACACGGGAA-3';

Acs14 forward: 5'-CATCCCTGGAGCAGATACTCT-3';

Acs14 reverse: 5'-TCACTTAGGATTCCTGGTCC-3'.

2.7. Cell culture

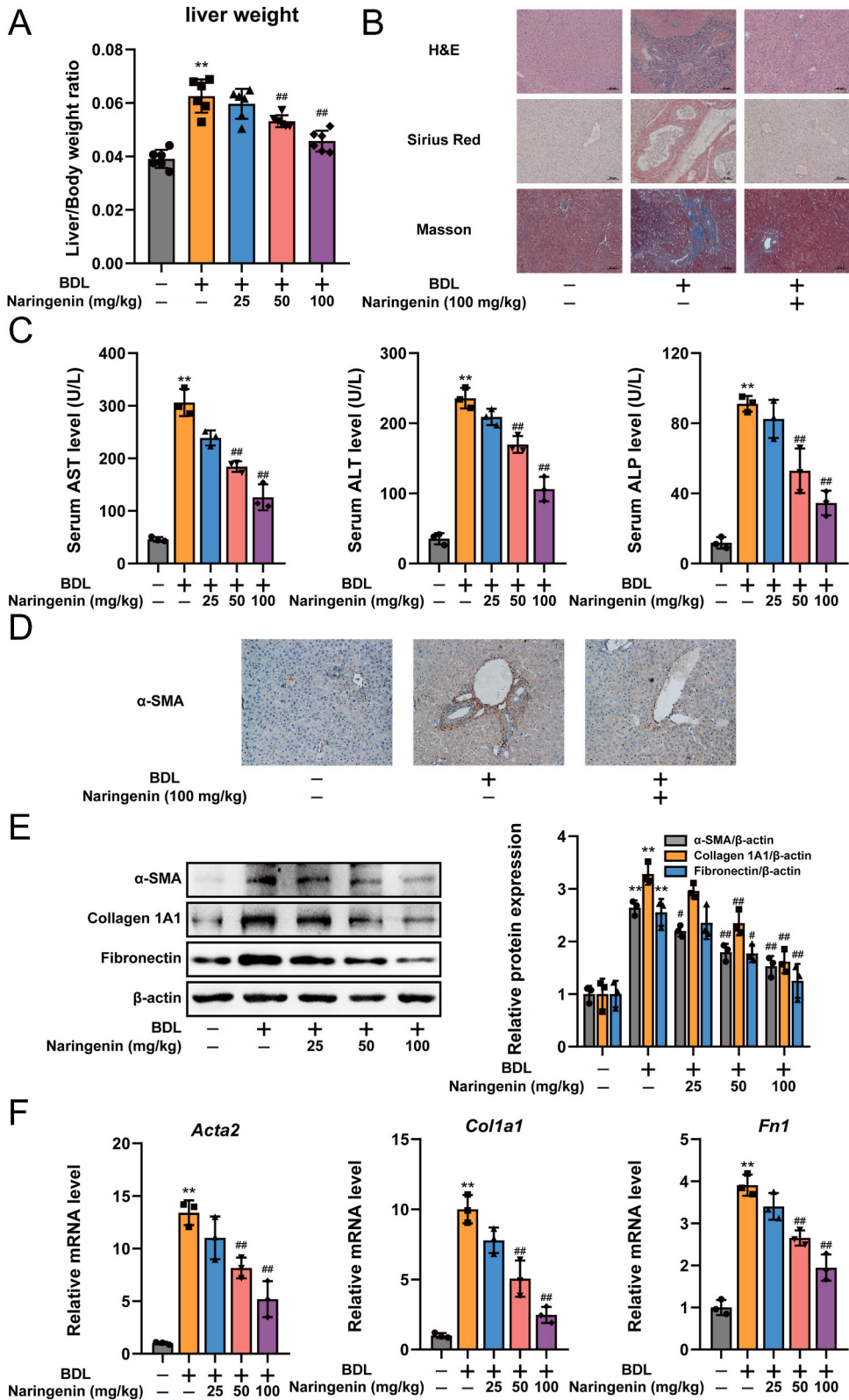
LX2 cells (sourced from the Cell Bank of the Shanghai Institute of Biochemistry and Cell Biology) were cultured in Dulbecco's modified Eagle's medium (DMEM) supplemented with 10% fetal bovine serum (FBS) obtained from Gibco, USA). The cells were maintained at 37 °C in a 5% CO₂ atmosphere.

2.8. Cell viability and cytotoxicity analyses

Cell viability and cytotoxicity were evaluated using the Cell Counting Kit-8 (CCK-8, #C0042, Beyotime, China) and lactate dehydrogenase (LDH) Release Assay Kit (#C0017, Beyotime, China), respectively, following the manufacturer's protocols. The CCK-8 assay provides a quantitative measurement of cell viability based on cellular metabolic activity, whereas the LDH Release Assay Kit allows the assessment of cytotoxicity by measuring the release of LDH into the culture medium.

2.9. Iron, Malondialdehyde, glutathione, lipid peroxidation assays

Iron levels were assessed using an iron assay kit (ab83366; Abcam). Malondialdehyde (MDA) was detected using an MDA Detection Kit (#A003-4-1, Jiancheng, China). A glutathione assay kit (BB-4711, BestBio) was used to determine the relative concentration of



(caption on next page)

Fig. 1. Naringenin alleviates liver fibrosis induced by bile duct ligation (BDL). (A) Liver-to-body weight ratio in mice from indicated group (n = 6). (B) Representative images, H&E, Sirius Red, Masson stains of liver in mice from indicated group. (Scale bars: 50 μ m). (C) Aspartate aminotransferase (AST), Alanine Aminotransferase (ALT), Alkaline Phosphatase (ALP) levels in the serum of liver in mice (n = 3). (D) Immunohistochemistry of α -SMA in the liver of BDL model mice. (Scale bars: 50 μ m). (E) Western blot analysis and semi-quantitation of the expression of α -SMA, Collagen 1A1 (Col1a1), Fibronectin (Fn1). β -actin served as the loading control (n = 3). (F) The mRNA levels of Acta2, Col1a1, Fn1 in liver tissues of the indicated mice group (n = 3). Data are presented as the mean \pm SD. ** P < 0.01 compared with normal mice; # P < 0.05, ## P < 0.01 compared with BDL mice. Uncropped gels and blots are in [Supplementary Fig. 1](#).

GSH. LPO was evaluated using the BODIPY 581/591 C11 Lipid Peroxidation Sensor from GlpBio (Montclair, CA, USA), which enables the measurement of lipid reactive oxygen species (ROS) levels. These assays collectively provided insights into the levels of iron, MDA, GSH, and LPO in the experimental samples.

2.10. Statistical analysis

Data derived from a minimum of three independent experiments were analyzed using the GraphPad Prism 8 software. The results were presented as the mean \pm standard deviation. Statistical evaluations were performed using one-way analysis of variance (ANOVA). Statistical significance was set at P < 0.05, indicating significant differences among experimental groups.

3. Results

3.1. Naringenin ameliorated hepatic fibrosis in BDL mice

The persistent cholestasis associated with BDL results in hepatocyte damage and enhanced ECM [32]. The liver-to-body weight ratio, which was markedly elevated in the BDL group, was effectively reduced by naringenin treatment (Fig. 1A). Histological examination revealed substantial inflammatory infiltration and hepatocyte necrosis in the livers of BDL mice. Sirius Red and Masson's trichrome staining further highlighted extensive collagen deposition. Naringenin treatment significantly attenuated these histological changes and reduced collagen accumulation, indicating the amelioration of liver fibrosis (Fig. 1B). Serum levels of key liver injury markers including AST, ALT, and ALP were markedly elevated in the BDL group. Naringenin treatment effectively reduced the levels of these serum markers, indicating its role in alleviating liver injury (Fig. 1C). The expression of α -SMA in the liver tissue of mice subjected to BDL showed a marked increase, which was significantly attenuated by naringenin treatment. (Fig. 1D). Western blot results also confirmed that Naringenin dose-dependently downregulated the expression of hepatic fibrosis-related proteins α -SMA, Collagen1A1 (Col1a1), and Fibronectin (Fn1) (Fig. 1E). Naringenin treatment significantly reduced the mRNA levels of these fibrogenic genes (Fig. 1F). Collectively, these findings strongly suggested that naringenin has a therapeutic effect in relieving liver fibrosis in BDL mouse models.

3.2. Naringenin suppressed HSCs viability and activation

Proliferation and activation of HSCs are central to ECM synthesis during liver fibrosis. Our investigations revealed that naringenin exerted time- and concentration-dependent effects on the viability of LX2 cells (Fig. 2A). Subsequently, concentrations of 10, 20, and 40 μ M were selected for further studies, where it was observed that naringenin, particularly at 20 and 40 μ M, significantly inhibited the viability of LX2 cells without affecting hepatocytes at the same concentrations (Fig. 2B and C). Further molecular analyses, including Western blot, demonstrated that naringenin downregulated the protein levels of key HSC activation markers such as α -SMA, Col1a1, and Fn1 (Fig. 2D). This inhibitory effect was further supported by a decrease in the mRNA levels of Acta2, Col1a1, and Fn1 as evidenced by real-time PCR (Fig. 2E). These findings collectively confirmed that naringenin robustly inhibited HSC activation.

3.3. Naringenin triggered HSCs ferroptosis

The induction of ferroptosis is a pivotal mechanism for inhibiting the activation of HSCs [33]. Ferroptosis is characterized by an intracellular iron overload and reduced GSH levels. To elucidate the mechanistic basis of the anti-fibrotic effect of naringenin, we examined its impact on these crucial events. As illustrated in Fig. 3A, compared to the control group, naringenin increased mitochondrial membrane density and decreased mitochondrial cristae. Moreover, naringenin induced iron overload in HSCs (Fig. 3B). A notable reduction was observed in GSH levels (Fig. 3C). Ferroptosis is typically associated with LPO, leading to MDA accumulation. Naringenin markedly increased the MDA and LPO levels (Fig. 3D and E). Western blotting showed that naringenin downregulated SLC7A11 and GPX4 and increased ACSL4 protein levels (Fig. 3F). In addition, naringenin treatment reduced Gpx4 mRNA levels and increased Ptg2 and Acs14 mRNA levels (Fig. 3G). Collectively, these findings suggested that naringenin induces ferroptosis in HSCs.

3.4. Naringenin inhibited HSCs activation via triggering ferroptosis

To determine the role of ferroptosis in the suppression of HSC activation by naringenin, we used the ferroptosis inhibitor ferrostatin-1 (Fer-1). Critically, Fer-1 inhibited intracellular iron overload, GSH reduction, MDA accumulation, and lipid peroxidation induced by naringenin (Fig. 4A-D). Subsequently, the activation markers of HSCs, including α -SMA, Col1a1, and Fn1, were assessed.

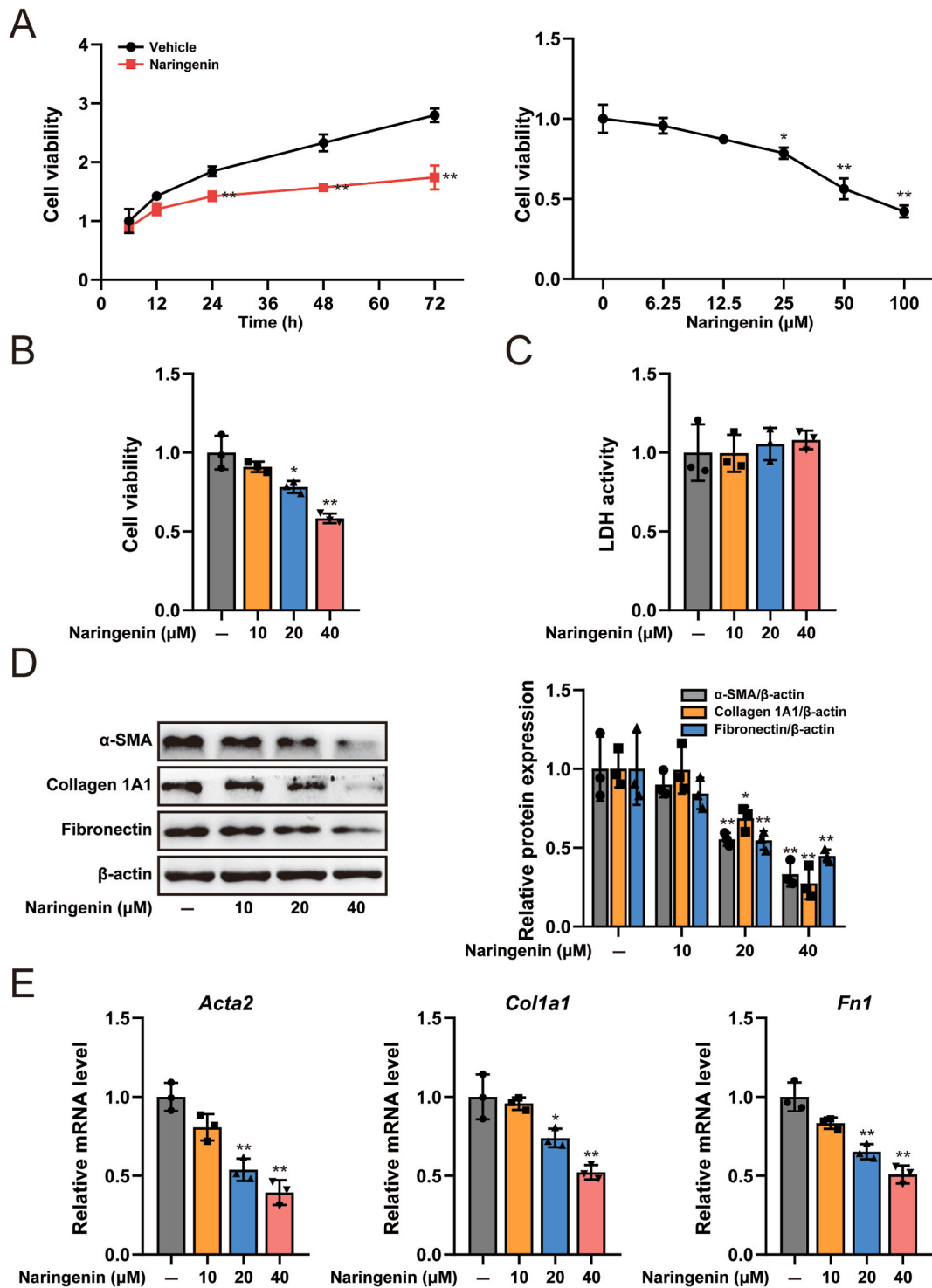


Fig. 2. Naringenin inhibits hepatic stellate cell (HSC) viability and activation. (A) LX2 cells were treated with naringenin (50 μM) for the indicated time or cells were treated with different concentrations of naringenin for 24 h, and cell viability was determined using CCK-8 assay. (B) LX2 cells were treated with indicated concentrations naringenin for the 24 h, and cell viability was determined using CCK-8 assay. (C) Cytotoxicity of AML-12 cells was assayed using an LDH kit. (D) Western blot analysis and semi-quantitation of the expression of α-SMA, Col1a1, and Fn1. β-actin served as the loading control. (E) The mRNA levels of Acta2, Col1a1, Fn1 in LX2 cells treated with naringenin. Data are presented as the mean ± SD (n = 3). * $P < 0.05$, ** $P < 0.01$ compared with control group. Uncropped gels and blots are in [Supplementary Fig. 2](#).

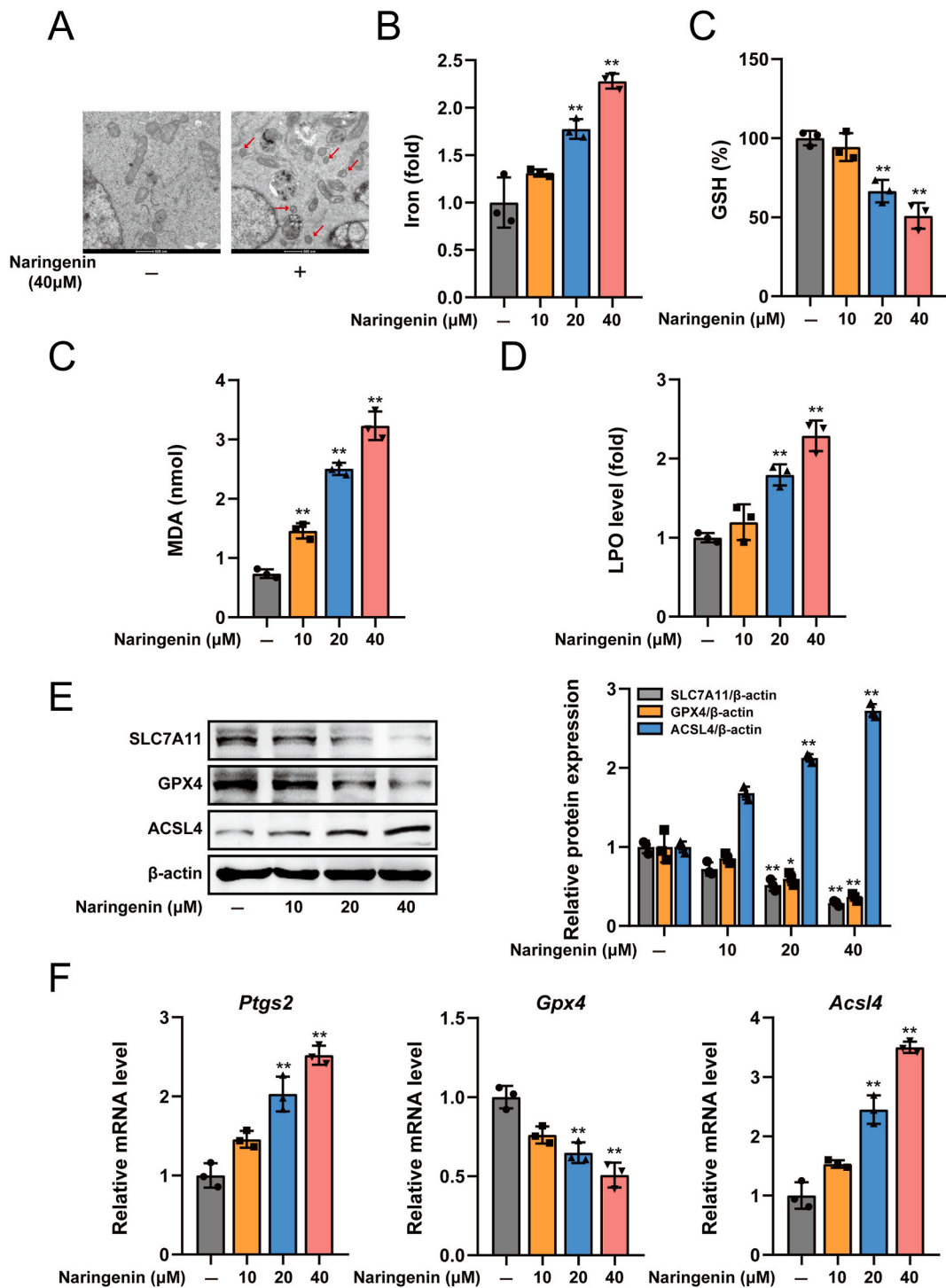


Fig. 3. Naringenin triggers HSC ferroptosis. (A) Morphology of nucleus and mitochondria examined using transmission electron microscopy. Red arrows indicate decreased mitochondrial cristae with increased membrane density. (B–E) LX2 cells treated with naringenin for 24 h. The levels of intracellular iron, GSH, MDA, and LPO were detected using a commercial kit. (F) Western blot analysis and semi-quantitation of the expression of SLC7A11, GPX4, ACSL4. β -actin served as the loading control. (G) The mRNA levels of *Ptgs2*, *Gpx4*, *Acs14* in LX2 cells treated with naringenin. Data are presented as the mean \pm SD (n = 3). * P < 0.05, ** P < 0.01 compared with control group. Uncropped gels and blots are in [Supplementary Fig. 3](#).

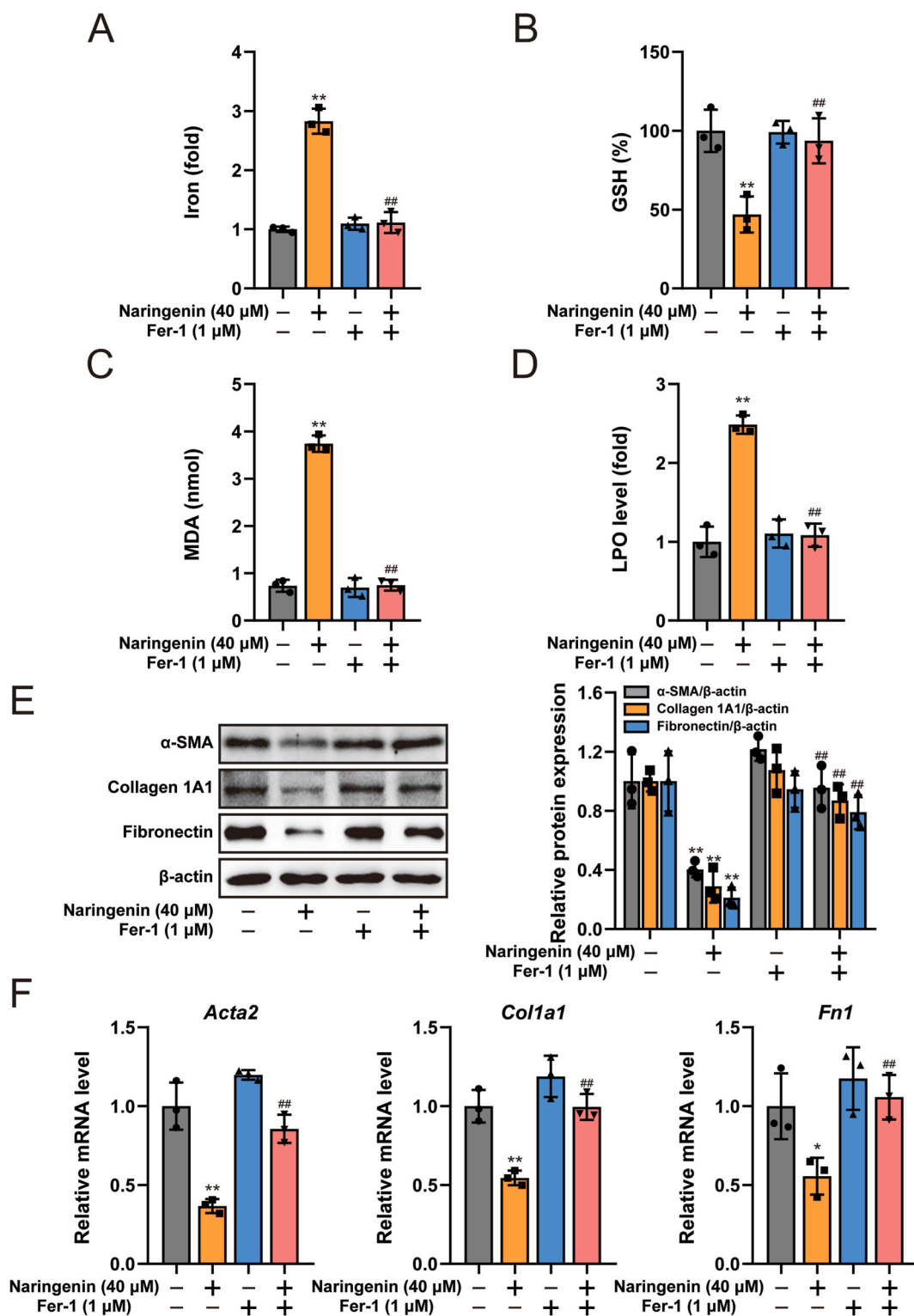
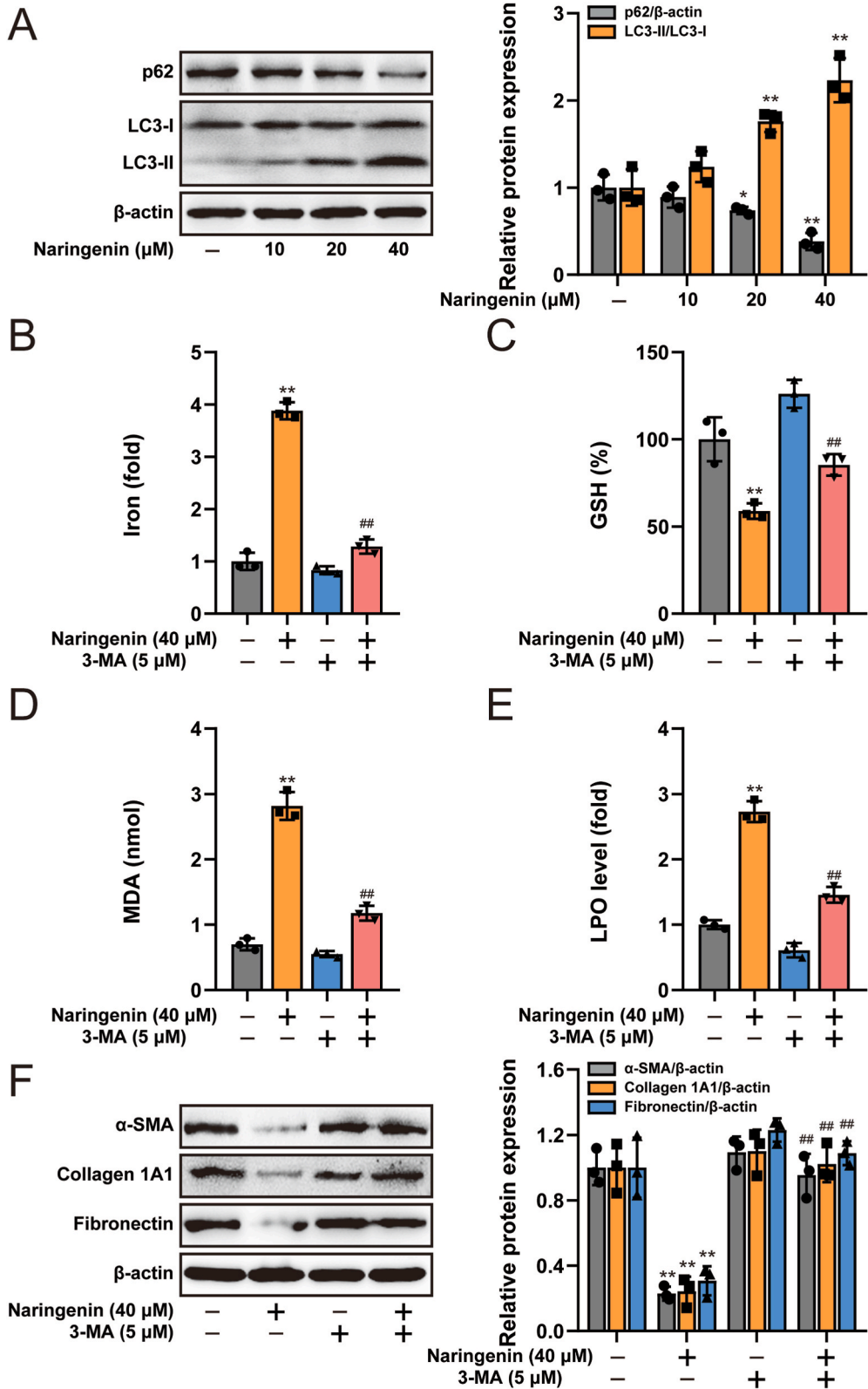


Fig. 4. Ferroptosis contributes to the inhibition of HSC activation by naringenin. (A–D) LX2 cells treated with Naringenin or ferrous sulfate. The levels of intracellular iron, glutathione (GSH), malonaldehyde (MDA), and lipid peroxidation (LPO) were detected using a commercial kit. (E) Western blot analysis and semi-quantitation of the expression of α -SMA, Col1a1, Fn1. β -actin served as the loading control. (E) The mRNA levels of Acta2, Col1a1, Fn1 in LX2 cells treated with naringenin or ferrous sulfate. Data are presented as the mean \pm SD ($n = 3$). * $P < 0.05$, ** $P < 0.01$ compared with control group; ## $P < 0.01$ compared with naringenin-treated group. Uncropped gels and blots are in [Supplementary Fig. 4](#).



(caption on next page)

Fig. 5. Autophagy is involved in naringenin-induced ferroptosis and inhibition of HSC. (A) Western blot analysis and semi-quantitation of the expression of p62 and LC3 in LX2 cells treated with naringenin. (B–E) LX2 cells treated with naringenin or 3-MA. The levels of intracellular iron, GSH, MDA, and LPO were detected using a commercial kit. (F) Western blot analysis and semi-quantitation of the expression of α -SMA, Col1a1, Fn1 in LX2 cells treated with naringenin or 3-MA. Data are presented as the mean \pm SD (n = 3). * P < 0.05, ** P < 0.01 compared with control group; ## P < 0.01 compared with naringenin-treated group. Uncropped gels and blots are in [Supplementary Fig. 5](#).

Interestingly, Fer-1 reversed the inhibitory effects of naringenin on HSC activation (Fig. 4E and F). These results confirm that naringenin inhibits HSC activation by inducing ferroptosis in HSCs, and this effect can be attenuated by Fer-1.

3.5. Naringenin induces ferroptosis by activating autophagy to alleviate the activation of HSCs

Autophagy regulates ferroptosis in several ways. To elucidate the molecular mechanisms underlying naringenin-induced ferroptosis, we initially assessed autophagy following naringenin treatment. The results showed that naringenin increased the expression of

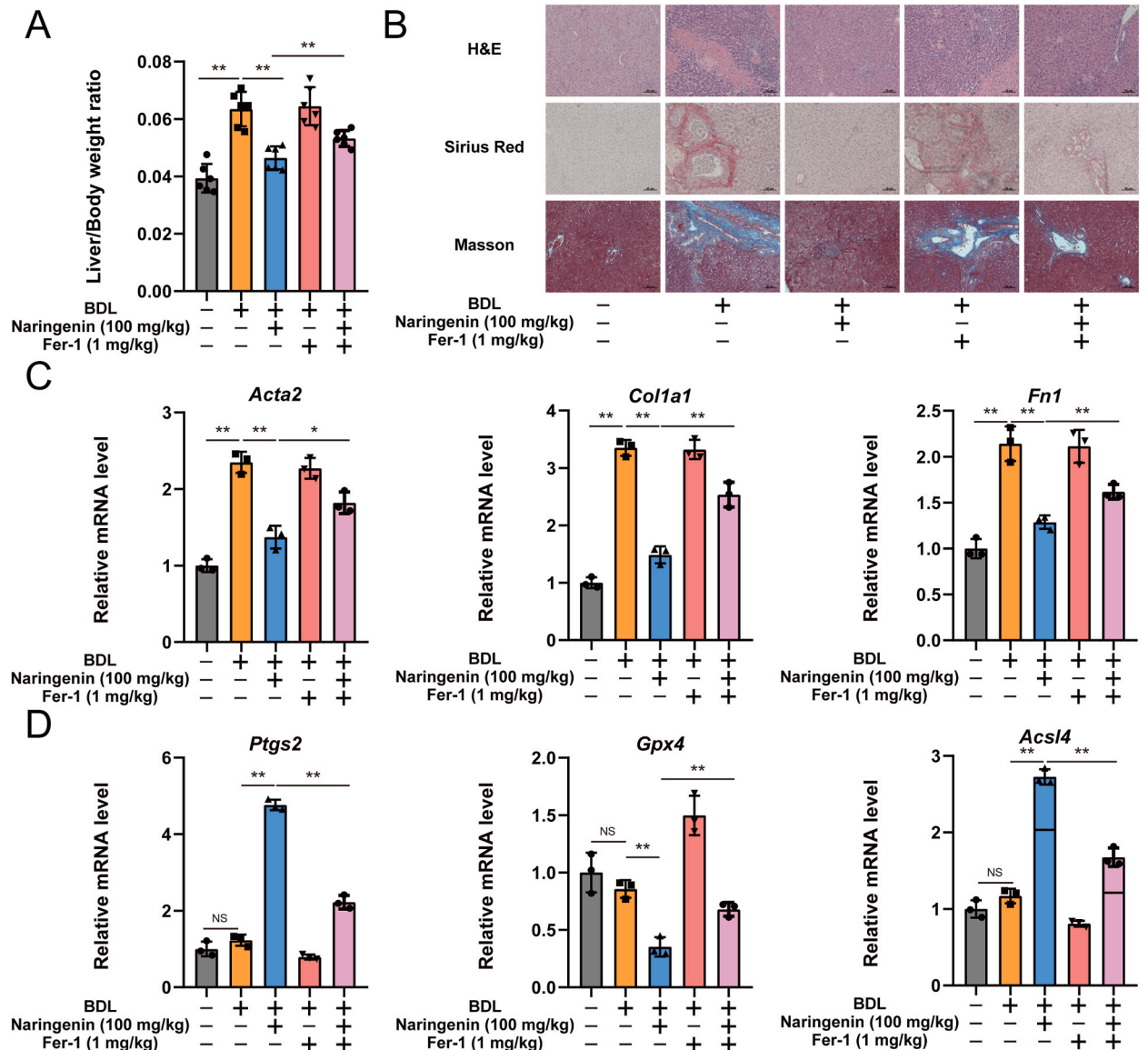


Fig. 6. Inhibition of ferroptosis attenuates anti-hepatic fibrosis effect of naringenin. (A) Liver-to-body weight ratio in mice from the indicated group (n = 6). (B) Representative images, H&E, Sirius Red, Masson stains of liver in mice from indicated group (Scale bars: 50 μ m). (C) The mRNA levels of Acta2, Col1a1, Fn1 in liver tissues of indicated group mice (n = 3). (D) The mRNA levels of Ptgs2, Gpx4, Acsl4 in liver tissues of indicated group mice (n = 3). Data are presented as the mean \pm SD. * P < 0.05, ** P < 0.01.

LC3-II while decreasing that of p62, suggesting increased autophagy in HSCs. (Fig. 5A). To substantiate the involvement of autophagy in naringenin-induced ferroptosis, we used the autophagy inhibitor, 3-MA. Interestingly, naringenin-induced iron overload, GSH decrease, MDA accumulation, and LPO were abolished by 3-MA (Fig. 5B-E). Subsequently, markers of HSC activation were examined. The results confirmed that the inhibitory effects of naringenin on α -SMA, Col1a1, and Fn1 were also annulled by 3-MA (Fig. 5F). These results suggested that naringenin induces ferroptosis and inhibits HSC activation by activating autophagy.

3.6. Suppression of ferroptosis attenuated the effect of naringenin against hepatic fibrosis

To evaluate the involvement of ferroptosis in liver fibrosis and the antifibrotic mechanisms of naringenin, Fer-1 was administered to BDL mouse model of liver fibrosis. Naringenin demonstrated a clear reduction in the liver-to-body weight ratio, indicating its therapeutic impact on liver fibrosis. However, the effect of naringenin was significantly diminished by the addition of Fer-1 (Fig. 6A). Moreover, naringenin significantly reduced the pathological changes in fibrotic morphology, whereas Fer-1 eliminated the antifibrotic effect of naringenin (Fig. 6B). The inhibitory effects of Naringenin on Acta2, Col1a1, and Fn1 mRNA levels were prevented by Fer-1 treatment (Fig. 6C). Additionally, Fer-1 reversed the naringenin-induced changes in the mRNA levels of ferroptosis-related genes

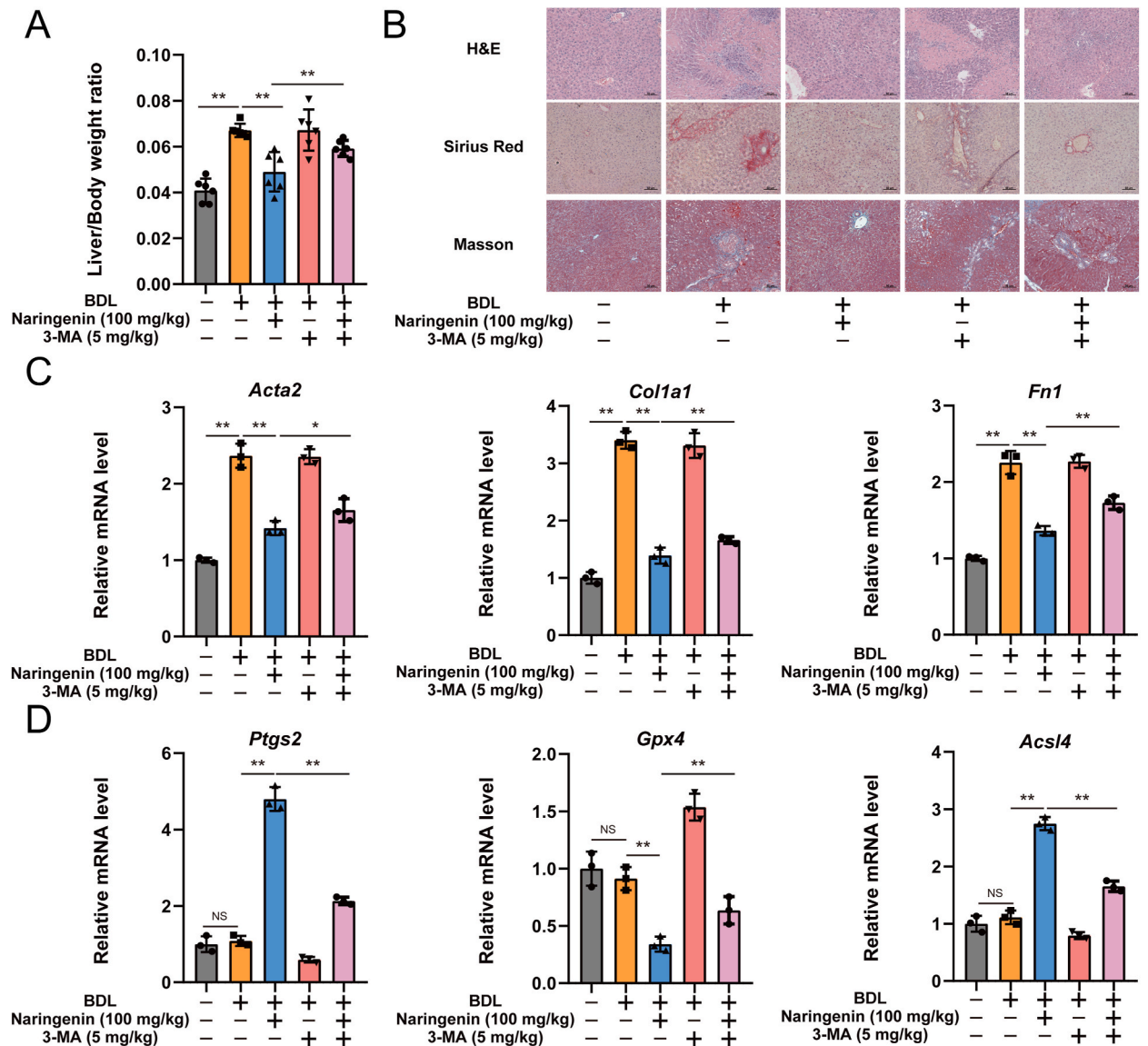


Fig. 7. Blockade of autophagy reverses the anti-hepatic fibrosis effect of Naringenin. (A) Liver-to-body weight ratio in mice from the indicated group (n = 6). (B) Representative images, H&E, Sirius Red, Masson stains of liver in mice from indicated group (Scale bars: 50 μ m). (C) The mRNA levels of Acta2, Col1a1, Fn1 in the liver tissues of mice from the indicated group (n = 3). (D) The mRNA levels of Ptg2, Gpx4, and Acs14 in liver tissues of indicated group mice (n = 3). Data are presented as the mean \pm SD. * P < 0.05, ** P < 0.01.

(Fig. 6D). Taken together, naringenin may inhibit liver fibrosis by inducing ferroptosis.

3.6.1. Blocking autophagy reversed the anti-hepatic fibrosis effect of naringenin

To elucidate the role of autophagy in the anti-fibrotic effects of naringenin, we used the autophagy inhibitor 3-MA. Naringenin significantly reduced the liver weight-to-body weight ratio, and blocking autophagy reversed this reduction in liver weight (Fig. 7A). More importantly, 3-MA reversed the antifibrotic effects of naringenin (Fig. 7B). The effect of naringenin on the mRNA levels of Acta2, Coll1a1, and Fn1 was reversed by 3-MA treatment (Fig. 7C). In addition, naringenin-induced increases in the mRNA levels of genes involved in ferroptosis were inhibited by blocking autophagy (Fig. 7D). In conclusion, blocking autophagy reversed the anti-hepatic fibrosis effects of naringenin.

4. Discussion

The activation and proliferation of HSCs is critical for the development of liver fibrosis [34]. Continuous liver injury triggers the differentiation of HSCs into activated myofibroblasts, fostering rapid proliferation and excessive collagen production, leading to the accumulation of extracellular matrix and eventual liver fibrosis [35]. Given the central role of HSCs, strategies targeting effective elimination of activated HSCs are crucial for therapeutic intervention [36]. Ferroptosis caused by abnormal iron metabolism is a novel form of programmed cell death. Several studies have investigated the relationship between ferroptosis and liver fibrosis. In mice, early treatment with erastin and sorafenib attenuates hepatic fibrosis through ferroptosis [37]. In other studies, natural products and their derivatives, such as artemether and artemisinin, have been shown to attenuate liver fibrosis through the induction of ferroptosis in HSCs [38]. Although studies have suggested that ferroptosis is a potential treatment for liver fibrosis, the exploration of safe and effective ferroptosis inducers is underway [39,40]. This is because ferroptosis activates HSCs and induces fibrosis. Iron is abundant in HSCs and is a prerequisite for ferroptotic cell death. Excessive hepatic iron deposition and ferroptosis potentiate acetaminophen-induced liver fibrosis in mice, which can be regressed by Fer-1 [41]. Therefore, ferroptosis promotes liver fibrosis. In this study, we found that naringenin mitigates BDL-induced liver fibrosis by inducing autophagy-associated ferroptosis.

Naringenin, with significant anti-inflammatory and antitumor properties [42–44], has been shown to reduce liver injury and ECM deposition in animal models of hepatotoxicity and CCl₄-induced liver fibrosis [28]. Our findings revealed that naringenin reduced HSC viability in a concentration- and time-dependent manner without affecting hepatocytes. Notably, naringenin-treated HSCs showed redox-active iron overload, GSH reduction, MDA production, and LPO. These results were consistent with the characteristics of ferroptosis. In order to investigate the mechanism of action of naringenin in liver fibrosis, we studied the ferroptosis of HSCs. To investigate the mechanism of action of naringenin in liver fibrosis, we studied HSC ferroptosis. Using the ferroptosis inhibitor Fer-1, we successfully reversed the inhibition of HSC activation and anti-fibrotic effects of naringenin. Collectively, these results indicated that naringenin exerts its antifibrotic effects by inducing ferroptosis in HSCs.

Previous studies have shown that autophagy is an important cellular process that regulates ferroptosis [20,45]. In particular, the discovery of ferritinophagy directly links autophagy and ferroptosis [46–48]. In addition to ferritinophagy, numerous studies have demonstrated that autophagy also indirectly modulates ferroptosis. For instance, Yang et al. highlighted that autophagic degradation of ARNTL can promote ferroptosis [49]. Additionally, the activation of ferroptosis enhances chaperone-mediated autophagy, leading to the degradation of GPX4, a key intracellular anti-lipid peroxidase [16,50,51]. Autophagy is a complex regulator with pro- and anti-fibrogenic properties in addition to ferroptosis. Yu et al. [52] reported that autophagy directly promotes fibrosis by inducing miR-29a. However, the ability of autophagy to inhibit fibrosis has been suggested by other studies [53]. In the present study, we observed that naringenin induced an increase in autophagy and that the autophagy inhibitor 3-MA significantly reversed the effects of naringenin in inducing ferroptosis and inhibiting HSC activation. These findings strongly suggested that naringenin-induced ferroptosis is intricately linked to autophagy activation.

Notably, our study adds to the existing literature by establishing the role of naringenin in the induction of ferroptosis in HSCs. Previous studies have demonstrated that naringenin induces apoptosis. Although ferroptosis and apoptosis are distinct mechanisms, emerging evidence suggests a potential interconnection between these two forms of cell death. Thus, it is essential to explore the mechanistic association between ferroptosis and apoptosis in the context of naringenin-induced cell death. In conclusion, our findings highlight that augmented autophagy induces ferroptosis following naringenin treatment, thus elucidating the interplay between autophagy and ferroptosis in liver fibrosis. The identification of autophagy activation opens novel avenues for investigating the anti-liver fibrosis mechanism of naringenin and highlights the scope for further research on drugs for the prevention and treatment of liver fibrosis.

5. Study limitation

Our study substantiates the efficacy of naringenin in alleviating liver fibrosis and elucidates the mechanism through which it inhibits the activation of HSCs through the induction of autophagy-dependent ferroptosis. However, further investigation is crucial to precisely understand how naringenin initiates autophagy. Additionally, it is noteworthy that our study exclusively used a BDL model to induce liver fibrosis and the lack of alternative liver fibrosis models to evaluate naringenin represents a limitation of the scope of our study. A more comprehensive assessment of diverse models would enhance the generalizability of our findings. Finally, before considering naringenin as a potential treatment for liver fibrosis in clinical studies, a thorough safety evaluation is a prerequisite. This step is crucial to establish the safety profile of a compound before it progresses to clinical trials.

Data availability statement

The data that support the findings of this study are available from the corresponding author upon reasonable request.

CRediT authorship contribution statement

Ting Yu: Conceptualization. **Xuejia Lu:** Data curation. **Yan Liang:** Formal analysis. **Lin Yang:** Methodology. **Yuehan Yin:** Software. **Hong Chen:** Writing – original draft.

Declaration of competing interest

The authors declare that they have no known competing financial interests or personal relationships that could have appeared to influence the work reported in this paper.

Acknowledgements

This study was supported by the Scientific Research Project of the Jiangsu Health Commission (M2021032).

Appendix A. Supplementary data

Supplementary data to this article can be found online at <https://doi.org/10.1016/j.heliyon.2024.e28865>.

References

- [1] R. Xu, Z. Zhang, F.S. Wang, Liver fibrosis: mechanisms of immune-mediated liver injury, *Cell. Mol. Immunol.* 9 (2012) 296–301, <https://doi.org/10.1038/cmi.2011.53>.
- [2] S. Lotersztajn, A. Mallat, Does CB-1 in hepatic stellate cells contribute to liver fibrosis? *J. Clin. Invest.* 132 (2022) <https://doi.org/10.1172/JCI155413>.
- [3] J. Zhang, et al., Sirt6 alleviated liver fibrosis by deacetylating conserved lysine 54 on Smad2 in hepatic stellate cells, *Hepatology* 73 (2021) 1140–1157, <https://doi.org/10.1002/hep.31418>.
- [4] K. Bottcher, M. Pinzani, Pathophysiology of liver fibrosis and the methodological barriers to the development of anti-fibrogenic agents, *Adv. Drug Deliv. Rev.* 121 (2017) 3–8, <https://doi.org/10.1016/j.addr.2017.05.016>.
- [5] R. Que, et al., Decursin ameliorates carbon tetrachloride-induced liver fibrosis by facilitating ferroptosis of hepatic stellate cells, *Biochem. Cell. Biol.* (2022), <https://doi.org/10.1139/bcb-2022-0027>.
- [6] S. Pu, et al., Inhibition of 5-lipoxygenase in hepatic stellate cells alleviates liver fibrosis, *Front. Pharmacol.* 12 (2021) 628583, <https://doi.org/10.3389/fphar.2021.628583>.
- [7] S. Sun, et al., Curcumin alleviates liver fibrosis by inducing endoplasmic reticulum stress-mediated necroptosis of hepatic stellate cells through Sirt1/NICD pathway, *PeerJ* 10 (2022) e13376, <https://doi.org/10.7717/peerj.13376>.
- [8] Y. Li, Y. Yang, Y. Yang, Multifaceted roles of ferroptosis in lung diseases, *Front. Mol. Biosci.* 9 (2022) 919187, <https://doi.org/10.3389/fmolb.2022.919187>.
- [9] F. Pan, et al., The critical role of ferroptosis in hepatocellular carcinoma, *Front. Cell Dev. Biol.* 10 (2022) 882571, <https://doi.org/10.3389/fcell.2022.882571>.
- [10] L. Magtanong, et al., Context-dependent regulation of ferroptosis sensitivity, *Cell Chem. Biol.* (2022), <https://doi.org/10.1016/j.chembiol.2022.06.004>.
- [11] W. Song, J. Chen, L. Wei, Ferroptosis in aortic dissection: cause or effect, *Pharmacol. Res.* 182 (2022) 106344, <https://doi.org/10.1016/j.phrs.2022.106344>.
- [12] K. Du, et al., Inhibiting xCT/SLC7A11 induces ferroptosis of myofibroblastic hepatic stellate cells but exacerbates chronic liver injury, *Liver Int.* 41 (2021) 2214–2227, <https://doi.org/10.1111/liv.14945>.
- [13] J. Li, et al., Tumor heterogeneity in autophagy-dependent ferroptosis, *Autophagy* 17 (2021) 3361–3374, <https://doi.org/10.1080/15548627.2021.1872241>.
- [14] Z. Li, et al., Engineering dual catalytic nanomedicine for autophagy-augmented and ferroptosis-involved cancer nanotherapy, *Biomaterials* 287 (2022) 121668, <https://doi.org/10.1016/j.biomaterials.2022.121668>.
- [15] J. Liu, et al., Autophagy-dependent ferroptosis: machinery and regulation, *Cell Chem. Biol.* 27 (2020) 420–435, <https://doi.org/10.1016/j.chembiol.2020.02.005>.
- [16] M. Ashrafizadeh, et al., Autophagy, anoikis, ferroptosis, necroptosis, and endoplasmic reticulum stress: potential applications in melanoma therapy, *J. Cell. Physiol.* 234 (2019) 19471–19479, <https://doi.org/10.1002/jcp.28740>.
- [17] W. Guo, Y. Zhao, H. Li, L. Lei, NCOA4-mediated ferritinophagy promoted inflammatory responses in periodontitis, *J. Periodontol. Res.* 56 (2021) 523–534, <https://doi.org/10.1111/jre.12852>.
- [18] Z. Luo, et al., HMG2A alleviates ferroptosis by promoting GPX4 expression in pancreatic cancer cells, *Cell Death Dis.* 15 (2024) 220, <https://doi.org/10.1038/s41419-024-06592-y>.
- [19] Y. Sun, et al., Fin56-induced ferroptosis is supported by autophagy-mediated GPX4 degradation and functions synergistically with mTOR inhibition to kill bladder cancer cells, *Cell Death Dis.* 12 (2021) 1028, <https://doi.org/10.1038/s41419-021-04306-2>.
- [20] Q. Peng, et al., Effect of autophagy on ferroptosis in foam cells via Nrf2, *Mol. Cell. Biochem.* 477 (2022) 1597–1606, <https://doi.org/10.1007/s11010-021-04347-3>.
- [21] X. Lin, et al., Focus on ferroptosis, pyroptosis, apoptosis and autophagy of vascular endothelial cells to the strategic targets for the treatment of atherosclerosis, *Arch. Biochem. Biophys.* 715 (2022) 109098, <https://doi.org/10.1016/j.abb.2021.109098>.
- [22] Z. Wu, et al., Chaperone-mediated autophagy is involved in the execution of ferroptosis, *Proc. Natl. Acad. Sci. U. S. A.* 116 (2019) 2996–3005, <https://doi.org/10.1073/pnas.1819728116>.
- [23] S. Chen, J.Y. Zhu, X. Zang, Y.Z. Zhai, The emerging role of ferroptosis in liver diseases, *Front. Cell Dev. Biol.* 9 (2021) 801365, <https://doi.org/10.3389/fcell.2021.801365>.
- [24] S. Park, et al., Naringenin and phytoestrogen 8-prenylnaringenin protect against islet dysfunction and inhibit apoptotic signaling in insulin-deficient diabetic mice, *Molecules* 27 (2022), <https://doi.org/10.3390/molecules27134227>.
- [25] M. Alimohammadi, et al., The effect of immunomodulatory properties of naringenin on the inhibition of inflammation and oxidative stress in autoimmune disease models: a systematic review and meta-analysis of preclinical evidence, *Inflamm. Res.* (2022), <https://doi.org/10.1007/s00011-022-01599-7>.

- [26] A. Taslidere, N.B. Turkmen, O. Ciftci, M. Aydin, Investigation into the protective effects of Naringenin in phthalates-induced reproductive damage, *Eur. Rev. Med. Pharmacol. Sci.* 26 (2022) 3419–3429, <https://doi.org/10.26355/eurrev.202205.28835>.
- [27] Z. Liu, X. Niu, J. Wang, Naringenin as a natural immunomodulator against T cell-mediated autoimmune diseases: literature review and network-based pharmacology study, *Crit. Rev. Food Sci. Nutr.* (2022) 1–18, <https://doi.org/10.1080/10408398.2022.2092054>.
- [28] L. Chen, et al., Naringenin is a potential immunomodulator for inhibiting liver fibrosis by inhibiting the cGAS-STING pathway, *J Clin Transl Hepatol* 11 (2023) 26–37, <https://doi.org/10.14218/JCTH.2022.00120>.
- [29] Z. Namkhah, et al., Does naringenin supplementation improve lipid profile, severity of hepatic steatosis and probability of liver fibrosis in overweight/obese patients with NAFLD? A randomised, double-blind, placebo-controlled, clinical trial, *Int. J. Clin. Pract.* 75 (2021) e14852, <https://doi.org/10.1111/ijcp.14852>.
- [30] C. Gartung, et al., Down-regulation of expression and function of the rat liver Na⁺/bile acid cotransporter in extrahepatic cholestasis, *Gastroenterology* 110 (1996) 199–209, <https://doi.org/10.1053/gast.1996.v110.pm8536857>.
- [31] E. Hernandez-Aquino, et al., Naringenin attenuates the progression of liver fibrosis via inactivation of hepatic stellate cells and profibrogenic pathways, *Eur. J. Pharmacol.* 865 (2019) 172730, <https://doi.org/10.1016/j.ejphar.2019.172730>.
- [32] N. Abdel-Rahman, M.H. Sharawy, N. Megahed, M.S. El-Awady, Vitamin D3 abates BDL-induced cholestasis and fibrosis in rats via regulating Hedgehog pathway, *Toxicol. Appl. Pharmacol.* 380 (2019) 114697, <https://doi.org/10.1016/j.taap.2019.114697>.
- [33] J. Gautheron, G.J. Gores, C.M.P. Rodrigues, Lytic cell death in metabolic liver disease, *J. Hepatol.* 73 (2020) 394–408, <https://doi.org/10.1016/j.jhep.2020.04.001>.
- [34] Z. Wu, et al., Regulatory long non-coding RNAs of hepatic stellate cells in liver fibrosis, *Exp. Ther. Med.* 21 (2021) 351, <https://doi.org/10.3892/etm.2021.9782> (Review).
- [35] D. Ezhilarasan, Hepatic stellate cells in the injured liver: perspectives beyond hepatic fibrosis, *J. Cell. Physiol.* 237 (2022) 436–449, <https://doi.org/10.1002/jcp.30582>.
- [36] X. Niu, et al., Research on promoting liver fibrosis injury by the targeted regulation of miR-202 for HGF to activate HSC, *Ir. J. Med. Sci.* 189 (2020) 1295–1304, <https://doi.org/10.1007/s11845-020-02210-w>.
- [37] Z. Zhang, et al., RNA-binding protein ZFP36/TTP protects against ferroptosis by regulating autophagy signaling pathway in hepatic stellate cells, *Autophagy* 16 (2020) 1482–1505, <https://doi.org/10.1080/15548627.2019.1687985>.
- [38] L. Wang, et al., P53-dependent induction of ferroptosis is required for artemether to alleviate carbon tetrachloride-induced liver fibrosis and hepatic stellate cell activation, *IUBMB Life* 71 (2019) 45–56, <https://doi.org/10.1002/iub.1895>.
- [39] J. Yi, et al., Berberine alleviates liver fibrosis through inducing ferrous redox to activate ROS-mediated hepatic stellate cells ferroptosis, *Cell Death Dis.* 7 (2021) 374, <https://doi.org/10.1038/s41420-021-00768-7>.
- [40] Z. Zhang, et al., Dihydroartemisinin alleviates hepatic fibrosis through inducing ferroptosis in hepatic stellate cells, *Biofactors* 47 (2021) 801–818, <https://doi.org/10.1002/biof.1764>.
- [41] M. Aldrovandi, M. Conrad, Ferroptosis: the good, the bad and the ugly, *Cell Res.* 30 (2020) 1061–1062, <https://doi.org/10.1038/s41422-020-00434-0>.
- [42] M. Motallebi, et al., Naringenin: a potential flavonoid phytochemical for cancer therapy, *Life Sci.* 305 (2022) 120752, <https://doi.org/10.1016/j.lfs.2022.120752>.
- [43] Y.X. Wu, et al., Naringenin regulates gut microbiota and SIRT1/PGC-1 α signaling pathway in rats with letrozole-induced polycystic ovary syndrome, *Biomed. Pharmacother.* 153 (2022) 113286, <https://doi.org/10.1016/j.biopha.2022.113286>.
- [44] Z. Calis, D. Dasdelen, A.K. Baltaci, R. Mogulkoc, Naringenin prevents inflammation, apoptosis, and DNA damage in potassium oxonate-induced hyperuricemia in rat liver tissue: roles of cytochrome C, NF-kappaB, caspase-3, and 8-hydroxydeoxyguanosine, *Metab. Syndr. Relat. Disord.* (2022), <https://doi.org/10.1089/met.2022.0028>.
- [45] Q. Guo, X. Zhang, T. Shen, X. Wang, Identification of autophagy- and ferroptosis-related lncRNAs functioned through immune-related pathways in head and neck squamous carcinoma, *Life* 11 (2021), <https://doi.org/10.3390/life11080835>.
- [46] Y.C. Liu, et al., Ferritinophagy induced ferroptosis in the management of cancer, *Cell. Oncol.* 47 (2024) 19–35, <https://doi.org/10.1007/s13402-023-00858-x>.
- [47] J. Jiang, Y. Ruan, X. Liu, J. Ma, H. Chen, Ferritinophagy is critical for deoxynivalenol-induced liver injury in mice, *J. Agric. Food Chem.* (2024), <https://doi.org/10.1021/acs.jafc.4c00556>.
- [48] J. Wang, et al., Ferritinophagy: research advance and clinical significance in cancers, *Cell Death Dis.* 9 (2023) 463, <https://doi.org/10.1038/s41420-023-01753-y>.
- [49] M. Yang, et al., Clockophagy is a novel selective autophagy process favoring ferroptosis, *Sci. Adv.* 5 (2019) eaaw2238, <https://doi.org/10.1126/sciadv.aaw2238>.
- [50] C. Li, et al., Mitochondrial DNA stress triggers autophagy-dependent ferroptotic death, *Autophagy* 17 (2021) 948–960, <https://doi.org/10.1080/15548627.2020.1739447>.
- [51] Z.M. Wu, et al., Chaperone-mediated autophagy is involved in the execution of ferroptosis, *P Natl Acad Sci USA* 116 (2019) 2996–3005, <https://doi.org/10.1073/pnas.1819728116>.
- [52] X. Yu, et al., Autophagy-related activation of hepatic stellate cells reduces cellular miR-29a by promoting its vesicular secretion, *Cell Mol Gastroenterol Hepatol* 13 (2022) 1701–1716, <https://doi.org/10.1016/j.jcmgh.2022.02.013>.
- [53] J. Lodder, et al., Macrophage autophagy protects against liver fibrosis in mice, *Autophagy* 11 (2015) 1280–1292, <https://doi.org/10.1080/15548627.2015.1058473>.